



# **Antibody Response against SRBC Immunosuppressed with Hydrocortisone Black Raspberry Extract Based Carbon Supported TiO<sub>2</sub> Crystal**

**K. Gayathiridevi<sup>1</sup> and G. Pasupathi<sup>2\*</sup>**

<sup>1</sup>*Department of Physics, Bharathidasan University Constituent College for Women,  
Orathanadu-614 625, India.*

<sup>2</sup>*Department of Physics, A.V.V.M. Sri Pushpam College (Autonomous), Poondi -613 503, India.*

## **Authors' contributions**

*This work was carried out in collaboration among two authors. Author KG designed the study performed the statistical analysis, wrote the protocol wrote the first draft of the manuscript. Author GP managed the literature searches and approved the final manuscript.*

## **Article Information**

DOI: 10.9734/EJMP/2019/v30i430193

### Editor(s):

- (1) Dr. Paola Angelini, Department of Chemistry, Biology and Biotechnology, University of Perugia, Italy.  
(2) Prof. Marcello Iriti, Professor of Plant Biology and Pathology, Department of Agricultural and Environmental Sciences, Milan State University, Italy.

### Reviewers:

- (1) Lígia Moura Burci, Faculdade Herrero, Brazil.  
(2) Gayatri C. Gawade, Bharati Vidyapeeth Deemed University Medical College, India.  
(3) Miloslav Milichovsky, University of Pardubice, Czechia.

Complete Peer review History: <http://www.sdiarticle4.com/review-history/53983>

**Original Research Article**

**Received 15 November 2019**  
**Accepted 17 January 2020**  
**Published 21 January 2020**

## **ABSTRACT**

As an titanium dioxide (TiO<sub>2</sub>) with carbon supported materials, particularly in anatase phase, have been extensively investigated and utilized in many technological applications due to its excellent physicochemical properties. This article summarizes the recent progress in growing carbon supported anatase TiO<sub>2</sub> crystals from the perspectives of Bridgemen technique. The Bridgmen technique is used to grow this crystal with TiO<sub>2</sub> directly dissolved with carbon sources and 10 mL of Black Raspberry, as well as the performance in various applications are largely determined by external surfaces exposed, and thus crystal shape engineering is paramount for this type of materials. Furthermore, the antibody response against SRBC immunosuppressed with Hydrocortisone in Mice Model is explained here. This Crystal growth technique is also highlighted

\*Corresponding author: E-mail: [gpasupathi123@gmail.com](mailto:gpasupathi123@gmail.com);

which would open a new field for the growth of single crystals with unique morphology. The objective of this study was to examine the effects of an antibody response against SRBC product containing on the induction of the Mice antibody response to various antigens, both systemically and in the gut. The Mice received subsequently were immunized with sheep red blood cells (SRBC) and bovine serum albumin (BSA) to evaluate antibody responses in serum or with tetanus toxoid (TT) to measure the antibody response in gut contents. Control groups received phosphate-buffered saline. Overall, BSA and SRBC induced a detectable antibody response.

**Keywords:** *Sheep red blood cells; X-ray diffractometer; Fourier transform infrared spectrometer; 10 mL of black raspberry and mice model.*

## 1. INTRODUCTION

Biomedical applications are exciting and, have made it a promising material for health care, especially treatment of diseases of antibacterial activity. For instance, based on its excellent photocatalytic activity, photoexcited TiO<sub>2</sub> demonstrates the capability to kill cancer cells effectively, and it can also be applied as a nucleic acid endonuclease, which is of vital importance to genetic engineering. The unique physicochemical properties are not only impacted by the intrinsic characteristics, but also by crystal shape, size, doping and polymorph. Because of the significant impact of crystal shape distributions, general methodologies for the prediction, measurement, and improvement of crystal shape are highly desired for product and process design. These topics have been studied for a long period, recent breakthroughs in theoretical and experimental. For the crystal growth of thermoelectric material by the Bridgeman technique the following requirements have to be fulfilled [1].

- (i). One end of the growth ampoule should be tapered.
- (ii). The growth ampoule should be moved with respect to the furnace to facilitate single crystal growth.
- (iii). The growth ampoule should be attached to a thin wire which is wound on a pulley, which in turn is fixed, to a clock motor.
- (iv). The diameter of the pulley should be chosen to get the optimum rate of movement of the growth ampoule.
- (v). The temperature of the furnace should be 100°C above the melting point of the material which is 585°C [2].

High-index facets have unique surface atomic structures, such as a high density of atomic steps, dangling bonds, kinks and ledges, that render the excellent capability in clean-energy and environmental applications. However, high-

index facets present high surface energy and thus grow much faster than the other facets; consequently, they diminish rapidly and disappear during crystal growth. So it is still challenging as well as attractive to synthesize tailored anatase TiO<sub>2</sub> crystals bound by high-index facets [3].

## 2. EXPERIMENTAL

Because the black raspberry is rich in anthocyanin pigments, it usually have very dark purple black fruits. The black raspberry is also closely related to the red raspberries, sharing the distinctively white underside of the leaves and but differing in the ripe fruit being black, and in the stems being more prickly. The black fruit makes them look like blackberries, though this is only superficial, with the taste being unique and not like either the red raspberry or the blackberry [4].

The binary compound was prepared by weighing the ultrahigh purity elements of 1% of 10 mL of Black Raspberry for the carbon sources supported Titanium chloride and in the appropriate quantities. They were powdered and mixed thoroughly in an agate mortar. The quartz tubes used for melting this material were pre-coated internally with pyrolytic graphite. The pyrolytic graphite coating is made by cracking high purity organic vapours (toluene or benzene) inside the tube at the temperature of 1100°C to avoid any reaction between tellurium and quartz.

Samples for electrical characterization were also prepared as described above. The furnace holding the sample was heated by means of a power amplifier. With raise in temperature the voltage developed is measured through high input impedance DC microvolt amplifier and the details of the measurement are given. The material was put into the quartz tube and it was sealed under high vacuum of 10 torr using a diffusion pump. One end of the quartz tube was

sharply tapered to facilitate single crystal growth [5]. This ampoule was mounted in the crystal growth set up and centered exactly in the furnace. The material was melted by raising the temperature of the furnace to 700°C and it was maintained at the temperature for 3 hrs to obtain a homogeneous melt. Then the clock motor was switched on to start the movement of the ampoule downwards. After the ampoule moved out of the furnace the power was switched off. The Phase purity of the material was examined by XRD (X-Ray Diffractometer) and no other phase was present. Spherical morphology was observed by using Scanning Electron Microscopy. The Variation of electrical resistance with temperature gradient was measured by four probe method. These points have been carefully taken for designing crystal growth experimental setup. The furnace used was made of kanthal wire (heating coil) externally wound on a alumina tube of 1.5 inches. The length of the furnace is considerably long to have long uniform hot zone. This was designed and fabricated in the laboratory. The temperature of the furnace is maintained to an accuracy of  $\pm 2^\circ\text{C}$ . The rate of movement of the ampoule was 10 mm / hr [6].

The X-ray powder diffractometer (XRD) experiments were measured on a Rigaku D/max-RB diffractometer with Ni-filtered graphite monochromatized  $\text{CuK}\alpha$  radiation ( $\lambda = 1.54056 \text{ \AA}$ ) under 40 kV, 30 mA and scanning between  $10^\circ$  to  $90^\circ(2\theta)$ . The functional groups in carbon supported with 10 mL of Black Raspberry  $\text{TiO}_2$  were graphed by Fourier transform infrared

spectrometer (FTIR). Photoluminescence Spectrometer (PL) measurements of the as synthesized products were carried out an F-4500KIMON Fluorescence spectrophotometer at room temperature with a Xe lamp as the excited light source.

### 3. RESULTS AND DISCUSSION

In general, diffraction peak from a lattice plane is labeled as Miller indices (hkl) and these indices are related to inter-atomic spacing or 'd' spacing. For an orthogonal system (ie,  $\alpha = \beta = \gamma = 90^\circ$ ), the 'd' spacing for any set of planes is given by the formula:

$$\frac{1}{d_{hkl}^2} = \frac{h^2}{a^2} + \frac{k^2}{b^2} + \frac{l^2}{c^2}$$

where, 'a', 'b' and 'c' are the cell edges.

The commonly accepted formula for particle size broadening is the Scherrer formula:

$$D = \frac{0.94 \lambda}{\beta \cos\theta} \quad (1)$$

where, 'D' is the crystallite size, 'β' is the full width at half maximum (FWHM) of the respective peak and 'θ' is the corresponding Bragg's angle [7].

The grown crystal has the size nearly equal to 45 nm.

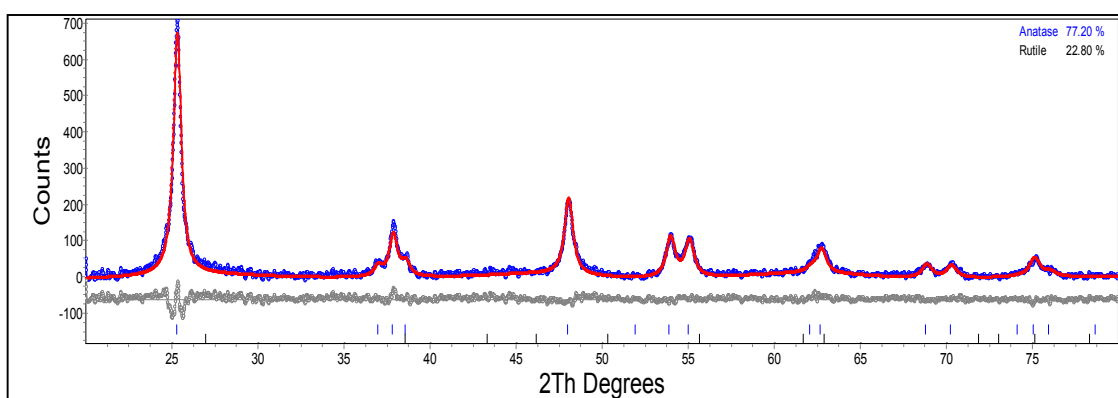


Fig. 1. Refined XRD pattern of carbon supported  $\text{TiO}_2$  single crystal

Table 1. Structural parameters of carbon supported  $\text{TiO}_2$  single crystal

hkl	Grystallite size D (nm)	Lattice parameter (Å)	Bandgap from PL (eV)
200	45.9	a = 3.777 c = 9.3613	3.154

### 3.1 Vicker's Micro Hardness

An important use of microhardness study is the possibility of making an indirect estimate of other mechanical characteristics of materials having a specific correlation with their hardness. Transparent and crack free crystals were chosen for hardness measurements. The crystal was then subjected to vickers microhardness test using HMV. 2T shimdazu instrument and the Vickers hardness number  $H_v$  is calculated using the relation [8].

$$H_v = 1.8544 \frac{P}{d^2} \quad (kg/mm^2) \quad (2)$$

Where  $d$  is the diagonal length of the indentation and  $P$  is the applied load in gram.

**Table 2. Micro hardness of carbon supported TiO<sub>2</sub> grown crystal**

load $p$ (g)	$H_v$ (kg/ mm <sup>2</sup> )
25	0.1115
50	0.1152
100	0.1723

The photoluminescence properties of carbon supported TiO<sub>2</sub> is having the wavelength of 388 nm and its band gap from this study 3.154 eV is detected. The band could be connected with electron~In PL spectra the bands at relaxation on uncharged oxygen interstitials<sup>1</sup> (3.154 eV relaxed electron affinity of uncharged O<sup>x</sup>). However, the luminescence of carbon supported TiO<sub>2</sub> single crystals this 388 nm (more than 3 eV) is useful for the optical applications which is shown in Fig. 2 [9,10].

TiO<sub>2</sub> shows the typical peaks at 522, 524, 1230, 1405, 1678 and 2219 cm<sup>-1</sup>, which correspond to the carbon, Titanium oxide groups hydroxyl groups, carboxyl groups and carbon oxygen bond, respectively are shown in Fig. 3 [11,12].

Intraperitoneal injection of Hydrocortisone to experimental Mice was also explained for DPPH (2,2-diphenyl-1-picrylhydrazyl) Free Radical Scavenging Activities. The free radical scavenging activity of the extracted fatty acid methyl esters from flower was examined *in vitro* using the 1,1-Diphenyl-2-picrylhydrazyl (DPPH) assay. The spectrophotometric assay was carried out according to the method previously described [13,14]. The DPPH free radical was freshly prepared at a 0.1 mM concentration in methanol and protected from light. Stock

solutions of the FAMES (1 mg / mL) was prepared and diluted to final concentration of 1000, 500, 300, 200, 100, 50 and 5 µg/ mL in methanol [15,16,17].

1 ml of 0.1 mM DPPH methanol solution was added to solutions of the sample as well as the standard (β-tocopherol) and incubated for 30 minutes in the dark. The absorbance was determined at 517 nm. Blank experiment was also carried out to determine the absorbance of DPPH before interacting with the sample. The percentage antioxidant activity (%AA) was obtained as percent DPPH radical scavenging, which was calculated using the equation:

$$\% AA = 100 \times [(Abs_{control} - Abs_{sample})] / (Abs_{control})$$

Where,  $Abs_{control}$  is the absorbance of the control and  $Abs_{sample}$  is the absorbance of the sample at 517 nm [18,17].

We explained that administration of hydrocortisone could decrease pain and analgesic requirements without significant adverse effects. Provision of adequate postoperative pain relief is of considerable importance. Several factors including patient demographics, nature of underlying disease, surgical factors, volume of residual gas, number of techniques were described to reduce post-laparoscopy pain including preincisional infiltration and intraperitoneal instillation of levobupivacaine, intraperitoneal ropivacaine and a gas drain, intraperitoneal levobupivacaine with epinephrine, intraperitoneal application of bupivacaine plus morphine, preincisional injection of bupivacaine. It has been suggested [19] that a high initial response, characteristic of high antibody lines, may preclude resources available for Mice anamnestic responses. Moreover, the observation that antigen dosages used for the initial inoculation influenced the responses to re-inoculation only in the low line would have implications for the effectiveness of vaccination programs involving stocks of differing immune competence [20].

Results of the present work are consistent with the report by Biozzi, et al. [17] who observed that their low SRBC antibody responder line of mice required a larger threshold dosage (100-fold) than the high line. Although the results indicating that line differences in primary antibody titers varied directly with SRBC dosage, which is not consistent with that reported in mice and for our lines include the threshold dosage for either line [19].

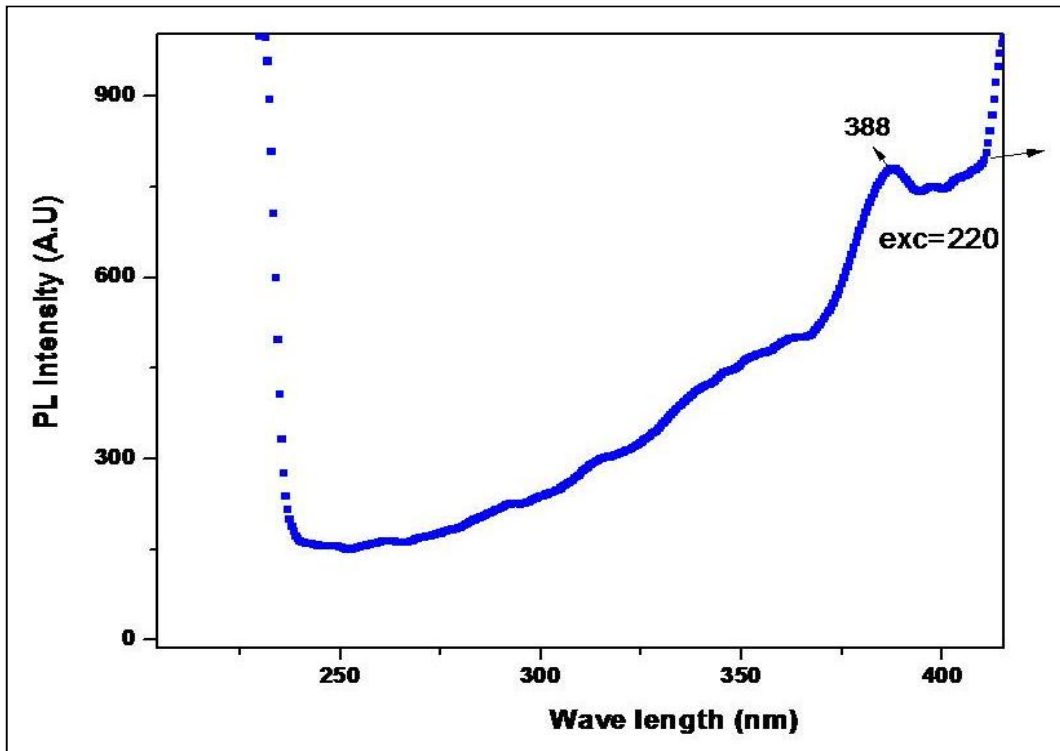


Fig. 2. Photoluminescence excitation spectra of carbon supported TiO<sub>2</sub> crystals

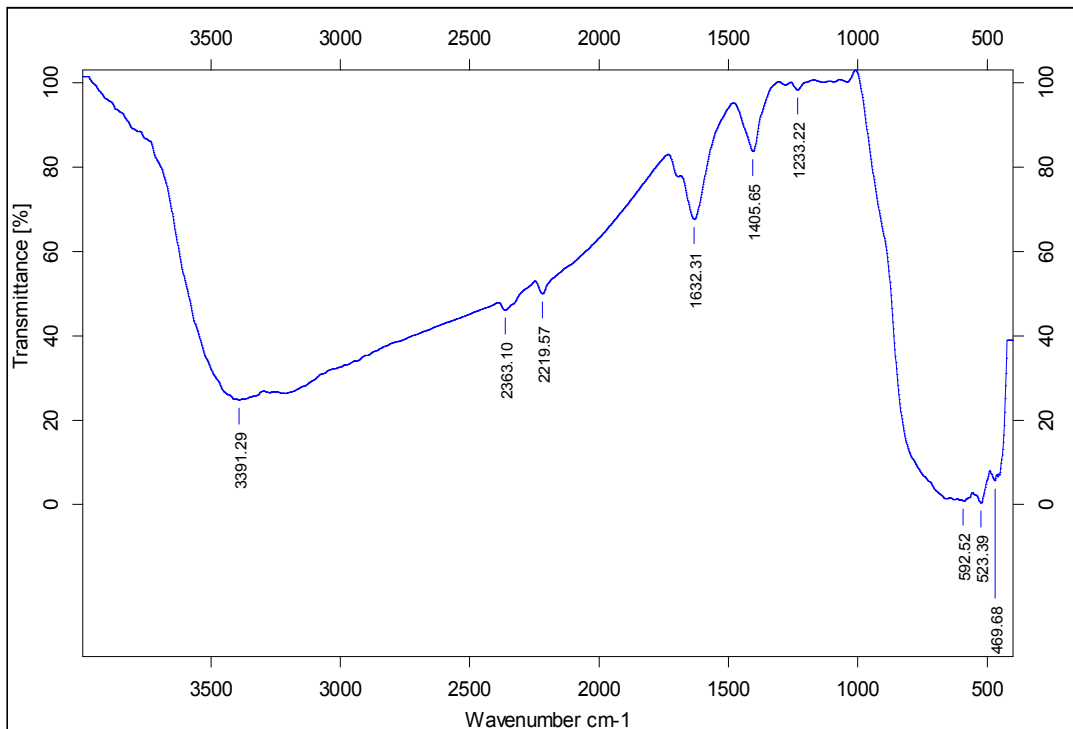


Fig. 3. FTIR analysis of carbon supported TiO<sub>2</sub> single crystals

**Table 3. Antibody response against SRBC immunosuppressed with hydrocortisone in mice model**

S. No	Groups	Spleen weight (g)	Cell yield/spleen	Level of serum biomarkers		Serum Triglycerides
				SGOT	SGPT U/L	
1.	Control	0.20±0.03	5.4±0.1×10 <sup>7</sup>	53.6 U/L	46.1	51.7 mgs/dl
2.	Hydrocortisone	0.16±0.03	3.4±1.7×10 <sup>7</sup>	61.4 U/L	43.4	54.1 mgs/dl
3.	Carbon supported TiO <sub>2</sub> crystal Supplemented Solvent	0.20±0.02	5.1±0.8×10 <sup>7</sup>	60.7 U/L	45.2	51.9 mgs/dl

**Table 4. DPPH assay for antioxidation studies**

S.No	Experiment (ml)	DPPH (ml)	Sample (ml) N1	OD at 517nm
1.	Blank	—	(0.5) Methanol	0.00
2.	Control	0.1	(0.5) Methanol	0.19
3.	Standard	1.0	—	0.51
4.	0.5	0.1	0.5	0.65
5.	1.0	0.1	1.0	0.95
6.	2.0	0.1	2.0	1.74



**Fig. 4. Experimental section of hydrocortisone**

#### 4. CONCLUSION

As comparison, the Bridgmen technique would be more attractive in view of the unique crystalline structures stemmed from nature. For example, the skeleton of a brittle star is composed of a single calcite crystal with regular inner pores which is derived from the biological organism. For biomedical applications, carbon supported TiO<sub>2</sub> crystals with tailored facets have offered a host of approaches to electrochemical biosensors, such as disease diagnosis and drug monitor. But more symmetric characterisations and other facets are important property which is very helpful for the biomedical applications of anatase 10 mL of

Black Raspberry carbon supported TiO<sub>2</sub> crystals. Almost all these are closely related to the surface properties or crystal geometries and thus, crystal shape engineering of 10 mL of Black Raspberry carbon supported anatase TiO<sub>2</sub> crystal is truly valuable in an attempt to give promising progress in biomedical applications.

#### CONSENT

It is not applicable.

#### ETHICAL APPROVAL

It is not applicable.

## COMPETING INTERESTS

Authors have declared that no competing interests exist.

## REFERENCES

1. Sootsman JR, Chung DY, Kanatzidis MG. *Angewandte Chemie International Edition*. 2009;48(46):8616-8639.
2. Tavrina TV, Rogacheva EI, Pinegin VI. *Moldavian Journal of the Physical Sciences*. 2005;4(4):430-434.
3. Kaviyarasu K, Geetha N, Kanimozhi K, Magdalane CM, Sivaranjani S, Ayeshamariam A, Kennedy J, Maza M. *In vitro* cytotoxicity effect and antibacterial performance of human lung epithelial cells A549 activity of zinc oxide doped TiO<sub>2</sub> nanocrystals: Investigation of bio-medical application by chemical method. *Materials Science and Engineering: C*. 2017;74:325-333.
4. Prabhavathi G, Saleem AM, Ayeshamariam A, Punithevelan N, Srinivasan MP, Jayachandran M. Fabrication and characterization of TiO<sub>2</sub>: rGO thin films on Si substrate by spin coating technique for the determination of sensitivity of methanol gas concentration.
5. Murugadoss K, Gayathiridevi K, Pasupathi G. Crystallization, structural and nonlinear optical studies on bithiourea lithium potassium sulphate single crystal. *Journal of Optics*. 2016;45(2):136-140.
6. Manjula N, Kaviyarasu K, Ayeshamariam A, Selvan G, Diallo A, Ramalingam G, Mohamed SB, Letsholathebe D, Jayachandran M. Structural, morphological and methanol sensing properties of jet nebulizer spray pyrolysis effect of TiO<sub>2</sub> doped SnO<sub>2</sub> thin film for removal of heavy metal ions. *Journal of Nanoelectronics and Optoelectronics*. 2018;13(10):1543-1551.
7. Adeosun CB, Olaseinde S, Opeifa AO, Atolani O. Essential oil from the stem bark of *Cordia sebestena* scavenges free radicals. *Journal of Acute Medicine*. 2013; 3(4):138-141.
8. Adeosun CB, Bamigbade OL, Osho A, Atolani O. Volatile composition of the leaf, flower and fruit of *Cordia sebestena* (L.). *Journal of Essential Oil Bearing Plants*. 2015;18(4):976-981.
9. Ramesh J, Pasupathi G, Mariappan R, Kumar VS, Ponnuswamy V. Structural and optical properties of Ni doped ZnO thin films using sol-gel dip coating technique. *Optik-International Journal for Light and Electron Optics*. 2013;124(15): 2023-2027.
10. Pasupathi G, Philominathan P. Growth, structural, optical and hardness studies of lithium potassium sulphate single crystals— an inorganic NLO material. *Journal of Minerals and Materials Characterization and Engineering*. 2012;11(09):904.
11. Subramanian S, Rajendiran G, Sekhar P, Gowri C, Govindarajulu P, Aruldas MM. Reproductive toxicity of chromium in adult bonnet monkeys (*Macaca radiata* Geoffrey). Reversible oxidative stress in the semen. *Toxicology and Applied Pharmacology*. 2006;215(3):237-249.
12. Shanmugam S, Gedanken A. Carbon-coated anatase TiO<sub>2</sub> nanocomposite as a high-performance electrocatalyst support. *Small*. 2007;3(7): 1189-1193.
13. Yan Y, Zhang X, Mao H, Huang Y, Ding Q, Pang X. Hydroxyapatite/gelatin functionalized graphene oxide composite coatings deposited on TiO<sub>2</sub> nanotube by electrochemical deposition for biomedical applications. *Applied Surface Science*. 2015;329:76-82.
14. Roguska A, Pisarek M, Andrzejczuk M, Dolata M, Lewandowska M, Janik-Czachor M. Characterization of a calcium phosphate-TiO<sub>2</sub> nanotube composite layer for biomedical applications. *Materials Science and Engineering: C*. 2011;31(5): 906-914.
15. Lai Y, Lin L, Pan F, Huang J, Song R, Huang Y, Lin C, Fuchs H, Chi L. Bioinspired patterning with extreme wettability contrast on TiO<sub>2</sub> nanotube array surface: A versatile platform for biomedical applications. *Small*. 2013;9(17):2945-2953.
16. Saleem AM, Rajasekar S, Kaviyarasu K, Perumalsamy R, Ayeshamariam A, Jayachandran M. Green combustion synthesis of CeO<sub>2</sub> and TiO<sub>2</sub> nanoparticles doped with same oxide materials of ZrO<sub>2</sub>: Investigation of *In vitro* assay with Antibiotic Resistant Bacterium (ARB) and anticancer effect. *European Journal of Medicinal Plants*. 2019;1-17.
17. Atolani O, Adeniyi O, Kayode OO, Adeosun CB. Direct preparation of fatty acid methyl esters and determination of in vitro antioxidant potential of lipid from fresh *Sebal causarium* Seed. *Journal of Applied Pharmaceutical Science*. 2015;5(03):024-028.

18. Saleem AM, Prabhavathi G, Karunanithy M, Ayeshamariam A, Jayachandran M. Green synthesis of nanoparticle by plant extracts—A new approach in nanoscience. *Journal of Bionano-science*. 2018;12(3): 401-407.
19. Biozzi G, Mouton D, Heumann AM, Bouthillier Y, Stiffel C, Mevel JC. Genetic analysis of antibody responsiveness to sheep erythrocytes in crosses between lines of mice selected for high or low antibody synthesis. *Immunology*. 1979; 36(3):427.
20. Boa-Amponsem K, Dunnington EA, Baker KS, Siegel PB. Diet and immunological memory of lines of white leghorn chickens divergently selected for antibody response to sheep red blood cells. *Poultry Science*. 1999;78 (2):165-170.

---

© 2019 Gayathiridevi and Pasupathi; This is an Open Access article distributed under the terms of the Creative Commons Attribution License (<http://creativecommons.org/licenses/by/4.0>), which permits unrestricted use, distribution, and reproduction in any medium, provided the original work is properly cited.

*Peer-review history:*  
*The peer review history for this paper can be accessed here:*  
<http://www.sdiarticle4.com/review-history/53983>